Mon. Not. R. Astron. Soc. **000**, 1–17 (2006) Printed 27 April 2007 (MN LATEX style file v2.2)

On the prevalence of radio–loud AGN in brightest cluster galaxies: implications for AGN heating of cooling flows

P. N. Best,[1⋆], A. von der Linden[2], G. Kauffmann[2], T. M. Heckman[3], C. R. Kaiser[4]
[1] *SUPA†, Institute for Astronomy, Royal Observatory Edinburgh, Blackford Hill, Edinburgh EH9 3HJ*
[2] *Max-Planck-Institut für Astrophysik, Karl-Schwarzschild-Str. 1, D-85748 Garching, Germany*
[3] *Department of Physics & Astronomy, The Johns Hopkins University, Baltimore, MD 21218, USA*
[4] *School of Physics & Astronomy, University of Southampton, Southampton SO17 1BJ*

27 April 2007

ABSTRACT

The prevalence of radio-loud AGN activity in present-day massive halos is determined using a sample of 625 nearby groups and clusters selected from the Sloan Digital Sky Survey. Brightest group and cluster galaxies (BCGs) are more likely to host a radio–loud AGN than other galaxies of the same stellar mass (by below a factor of two at a stellar mass of $\sim 5 \times 10^{11} M_{\odot}$, but rising to over an order of magnitude below $10^{11} M_{\odot}$). The distribution of radio luminosities for BCGs does not depend on mass, however, and is similar to that of field galaxies of the same stellar mass. Neither the radio–loud fraction nor the radio luminosity distribution of BCGs depends strongly on the velocity dispersion of the host cluster. The radio-AGN fraction is also studied as a function of distance from the cluster centre. Only within 0.2 r_{200} do cluster galaxies exhibit an enhanced likelihood of radio–loud AGN activity, which approaches that of the BCGs. In contrast to the radio properties, the fraction of galaxies with optical emission–line AGN activity is suppressed within r_{200} in groups and clusters, decreasing monotonically towards the cluster centre.

It is argued that the radio–loud AGN properties of both BCGs and non-BCGs can naturally be explained if this activity is fuelled by cooling from hot gas surrounding the galaxy. Using observational estimates of the mechanical output of the radio jets, the time–averaged energy output associated with recurrent radio source activity is estimated for all group / cluster galaxies. Within the cooling radius of the cluster, the radio–mode heating associated with the BCG dominates over that of all other galaxies combined. The scaling between total radio–AGN energy output and cluster velocity dispersion is observed to be considerably shallower than the $\sim \sigma_v^4$ scaling of the radiative cooling rate. Thus, unless either the mechanical–to–radio luminosity ratio or the efficiency of converting AGN mechanical energy into heating increases by 2–3 orders of magnitude between groups and rich clusters, radio–mode heating will not balance radiative cooling in systems of all masses. In groups, radio–AGN heating probably overcompensates the radiative cooling losses, and this may account for the observed entropy floor in these systems. In the most massive clusters, an additional heating process (most likely thermal conduction) may be required to supplement the AGN heating.

Key words: galaxies: active — radio continuum: galaxies — galaxies: clusters: general — cooling flows — X-rays: galaxies: clusters

1 INTRODUCTION

Brightest cluster galaxies (hereafter BCGs) occupy a unique position at the centre of the gravitational potential well of clusters of galaxies. They are amongst the most luminous galaxies in the Universe, up to ten times brighter than typical elliptical galaxies, with large characteristic radii (tens of kpc; e.g. Schombert 1986) and, in some cases (the 'cD' galaxies; e.g. Oemler 1976), diffuse envelopes which can extend hundreds of kpc. The properties of BCGs are found to be correlated with those of their surrounding clusters (e.g. Edge 1991; Lin & Mohr 2004; Brough et al. 2005), and the formation history of BCG and cD galaxies is believed to be

⋆ Email: pnb@roe.ac.uk
† Scottish Universities Physics Alliance

distinct from that of other elliptical galaxies, due to their special location (e.g. Bernstein & Bhavsar 2001; De Lucia & Blaizot 2006, and references therein). They are also offset from the standard scaling relations of early–type galaxies (e.g. von der Linden et al. 2006).

Brightest cluster galaxies have long been recognised to show different radio properties to other cluster galaxies, being much more likely to be radio–luminous than other non–dominant cluster ellipticals (e.g. Burns et al. 1981; Valentijn & Bijleveld 1983; Burns 1990). This radio–loud AGN activity in BCGs has been proposed as a potential solution to the cooling–flow problem. Gas in the central regions of clusters of galaxies often has radiative cooling timescales very much shorter than the Hubble time and, in the absence of a heating source, a cooling flow would be expected to develop, whereby the temperature in the central regions of the cluster drops and gas flows inwards at rates of up to $\sim 1000 M_{\odot}\,\mathrm{yr}^{-1}$ (see Fabian 1994, for a review). However, recent XMM-Newton and Chandra observations of cooling flow clusters have shown that the temperature of cluster cores does not fall below $\sim 30\%$ of that at large radii, and that the amount of cooling gas is only about 10% of that predicted for a classical cooling flow (e.g. Peterson et al. 2001; David et al. 2001; Tamura et al. 2001; Kaastra et al. 2001). This implies that some heating source must balance the radiative cooling losses, preventing the gas from cooling further.

Heating by radio sources associated with the BCGs has gained popularity in recent years, as X–ray observations have revealed bubbles and cavities in the hot intracluster medium of some clusters, coincident with the lobes of the radio sources (e.g. Böhringer et al. 1993; Carilli et al. 1994; McNamara et al. 2000; Fabian et al. 2000; Blanton et al. 2001). These are regions where relativistic radio plasma has displaced the intracluster gas, creating a low–density bubble of material in approximate pressure balance with the surrounding medium, which then rises buoyantly and expands. Hydrodynamic simulations have been able to reproduce bubbles with properties similar to those observed (e.g. Churazov et al. 2001; Quilis et al. 2001; Brüggen & Kaiser 2002; Brüggen 2003) and have also shown that, provided that radio source activity is recurrent, the total energy provided by AGN activity can be sufficient to balance the cooling radiation losses through repeated production of jets, buoyant bubbles and associated shocks (e.g. Dalla Vecchia et al. 2004; Brüggen et al. 2005; Nusser et al. 2006). Other authors (e.g. Omma et al. 2004; Brighenti & Mathews 2006) have argued that momentum–driven jets are an alternative means of distributing AGN energy throughout the intracluster medium.

Very deep Chandra observations of the Perseus and Virgo clusters (Fabian et al. 2003; Fabian et al. 2006; Forman et al. 2005, 2006) have revealed the presence of approximately spherical weak shock waves in these clusters, extending out to several tens of kpc radius. Fabian et al. (2003) argued that these 'ripples' are excited by the expanding radio bubbles, and that dissipation of their energy can provide a quasi–continuous heating of the X–ray gas (see also Ruszkowski et al. 2004). Fujita & Suzuki (2005) and Mathews et al. (2006) argued, however, that if all of the wave dissipation occurs at the shock front then too much of the heat is deposited in the inner regions of the cluster, and not enough out at the cooling radius, leading to temperature profiles at variance with observations. Nusser et al. (2006) suggested that a natural solution to this problem is to consider the heating effects of AGN activity from all cluster galaxies, not only BCGs. More recently, Fabian et al. (2006) showed that the shocks occurring in the Perseus cluster are isothermal, meaning that thermal conduction must be important in mediating the shock. They argue that this prevents the accumulation of hot shocked gas in the inner regions, and that the energy of the waves can be dissipated at larger radii by viscous effects.

One critical question for all of these models is whether the heating generated by an episode of radio–loud AGN activity is sufficient, during its lifetime, to offset the radiative cooling losses of the cluster. Viewed in terms of the radio bubbles (which are widely considered to be the driving force behind the shock and sound waves), for some clusters the (pV) energy contained within the evacuated bubbles has been shown to be sufficient to balance the cooling losses, at least for a short period of time (a few $\times 10^7$ yr; e.g. Fabian et al. 2003; Bîrzan et al. 2004; Dunn et al. 2005). However, Bîrzan et al. (2004) showed that this is not true for about half of the clusters they studied (see also Rafferty et al. 2006). Nusser et al. (2006) and others have argued that the mechanical energy injected into the cluster by weak shocks may be up to an order of magnitude larger than pV, which would ease this problem. An alternative possibility is that the heat balance occurs in a quasi–static manner, with recurrent low luminosity radio activity being punctuated by occasional major eruptions supplying much more energy (Kaiser & Binney 2003).

A second important question is what the duty cycle of this AGN activity is. The duty cycle determines the rate of production of radio bubbles, or equivalently, the timescale between the sound wave 'ripples', and hence is required to calculate the time–averaged heating rate associated with AGN activity. Burns (1990) showed that as many as 70% of cD galaxies at the centre of cooling flow clusters are radio–loud, but this result was based on a sample of only 14 such systems, and not all BCGs are cD galaxies.

Recently, Best et al. (2005) used data from the Sloan Digital Sky Survey (SDSS; York et al. 2000; Stoughton et al. 2002) to investigate the origin of radio–loud AGN activity, and found that the dominant factor which determined whether or not a galaxy is radio–loud is its mass: the fraction of galaxies which were found to host radio–loud AGN scaled as $M_*^{2.5}$ or $M_{\rm BH}^{1.6}$, where M_* and $M_{\rm BH}$ are the stellar and black hole masses of the galaxy, respectively. The distribution of radio luminosities was found to be the same regardless of the galaxy mass. Combining these results with a conversion between radio luminosity and the mechanical energy supplied by a jet to its surroundings (as estimated by Bîrzan et al. 2004), Best et al. (2006) estimated the time–averaged mechanical luminosity output associated with radio source activity for each galaxy, as a function of its mass. They found that, for elliptical galaxies of all masses, the time averaged radio heating almost exactly balanced the radiative cooling losses from the hot haloes of the ellipticals. They argued that the radio AGN feedback may therefore play a critical role in galaxy formation, preventing further cooling of gas onto elliptical galaxies and thus explaining why these galaxies are old and red (see also Benson et al. 2003; Scan-

napieco et al. 2005; Croton et al. 2006; Bower et al. 2006; Cattaneo et al. 2006).

Best et al. (2006) also concluded that, unless brightest cluster galaxies showed a different mode of radio activity to that of ordinary elliptical galaxies, then they could not provide sufficient heating to balance the cooling in clusters of galaxies. As discussed above, BCGs *are* found to be radio–luminous much more frequently than other cluster ellipticals, but the strong mass dependence of the radio–loud AGN fraction found by Best et al. (2005) means that this may solely be due to their very much higher masses. The goal of the current paper is therefore to investigate this issue, by determining both the radio–loud fraction, and the distribution of radio luminosities, for a large sample of brightest group and cluster galaxies with a wide range of masses and host group / cluster properties. This will then ascertain the importance of radio–AGN heating in clusters. A secondary goal of the paper is to investigate the role that non–BCG cluster galaxies may have in heating the intracluster medium.

The layout of the paper is as follows. Section 2 describes the various data samples that are used for this analysis. An analysis of the radio properties of brightest group and cluster galaxies is carried out in Section 3, while Section 4 investigates the radio properties of the other group and cluster galaxies. These are compared against signatures of optical AGN activity in Section 5. The implications of these results for the origin and fuelling of low luminosity radio source activity are discussed in Section 6. In Section 7 the radio–AGN heating rates are estimated in clusters and groups across a wide range of masses, and compared these with the radiative cooling rates. The implications of these results for AGN heating of cooling flows are discussed in Section 8, and conclusions are drawn in Section 9. Throughout the paper, the cosmological parameters are assumed to have values of $\Omega_m = 0.3$, $\Omega_\Lambda = 0.7$, and $H_0 = 70\,\mathrm{km\,s^{-1}Mpc^{-1}}$.

2 SAMPLE SELECTION

2.1 Definition of the galaxy samples

The Sloan Digital Sky Survey (York et al. 2000; Stoughton et al. 2002) is a five-band photometric and spectroscopic survey which will ultimately cover about a quarter of the extragalactic sky; the fourth data release of this survey (DR4; Adelman-McCarthy et al. 2006) includes spectroscopy of over half a million objects. The parent sample for the current study is drawn from the 'main galaxy sample' (Strauss et al. 2002) of the SDSS DR4, comprising those galaxies with magnitudes in the range $14.5 < r < 17.77$. The spectra of these galaxies have been used to derive a large number of physical properties, with catalogues of measured and derived parameters being publically available (see http://www.mpa-garching.mpg.de/SDSS/).

Miller et al. (2005) have used the SDSS data to identify clusters of galaxies as overdensities in a seven-dimensional space of position and colour. This 'C4' cluster catalogue is currently available for DR3, and identifies 1106 clusters with redshifts $0.02 < z < 0.16$. Miller et al. also identify two candidate brightest cluster galaxies for each of their clusters: the 'mean galaxy' is that closest to the peak of the galaxy density field, and the 'brightest galaxy' is the brightest spectroscopically confirmed cluster member with a projected position within $500h^{-1}$kpc (where $h = H_0/100\,\mathrm{km\,s^{-1}Mpc^{-1}}$) of that density peak and a redshift within four times the velocity dispersion of the mean cluster redshift. In many cases, however, neither of these turns out to be the true BCG (see von der Linden et al. 2006). For example, in about 30% of dense clusters, the BCG is not included in the spectroscopic data, due to the problems of fibre collisions, and so is missed by the C4 catalogue.

In a companion paper, von der Linden et al. (2006) have re-analysed the C4 cluster catalogue in order to provide a robust sample of clusters with well–defined BCGs. The reader is referred to that paper for a detailed discussion of how the cluster sample and BCGs were defined. In brief, the sample was first restricted to the 833 C4 clusters with redshifts $z < 0.1$. The brightest cluster galaxies were then identified using all available information (magnitude, colour, morphology, redshift if in the spectroscopic sample), together with visual inspection of colour images of the clusters (see von der Linden et al. for details). During this process, clusters which were identified to be substructures of larger clusters were removed from the sample, as were those for which an iterative algorithm to determine the cluster redshift, velocity dispersion (σ_v) and virial radius (r_{200}) either did not converge or retained three or fewer galaxies within $3\sigma_\mathrm{v}$ and $1r_{200}$ of the cluster centre. This resulted in a final sample of 625 systems, for which the size, velocity dispersion, BCG and cluster membership were all well determined. It turns out that some of these systems have velocity dispersions which indicate that they are galaxy groups rather than clusters; the terms 'cluster' and 'brightest cluster galaxy' are used loosely in this paper, to include both clusters and groups.

A further critical re–analysis carried out by von der Linden et al. (2006) has been to correct the SDSS photometry for these BCGs. The SDSS photometry systematically underestimates the luminosities of nearby large galaxies, particularly in cluster environments, because it overestimates the level of sky background (Bernardi et al. 2006; Lauer et al. 2006; von der Linden et al. 2006). This then leads to underestimates of the galaxy mass, which would impact upon the current studies. von der Linden et al. derived a method to correct the photometry for this sky over-subtraction; their method uses both the 'local' and 'global' sky estimates provided by the SDSS pipeline, combined according to a weighted ratio of the luminosity of the galaxy to that of its neighbouring galaxies. They show that this method is successful in reproducing magnitudes which match with independent measurements (see their paper for more details).

In the current paper, the 'brightest cluster galaxy' sample generally corresponds to the 625 BCGs defined from this sample of clusters. In 141 of these clusters, however, the BCG is not contained within the spectroscopic catalogue; therefore, where comparison is being made with properties derived from spectroscopic observations (e.g. emission line strengths), the sample is restricted to only those 484 BCGs with spectroscopic data. Since the BCGs with only photometric data have generally been excluded from the spectroscopic sample due to random effects (especially fibre collisions) it is not expected that this will produce any significant bias in the sample.

The results for the BCGs are compared with those of 'all galaxies'. The 'all galaxy' sample corresponds to those

galaxies within the main galaxy sample of the SDSS DR4 release, with redshifts $0.02 < z < 0.1$; these redshift cuts match those applied to the cluster catalogue, and von der Linden et al. have also applied their photometric correction method to these galaxies in an equivalent way. The all galaxy sample is discussed by von der Linden et al.: it includes a mix of galaxy properties, in a wide range of environments, but in the luminosity range where the sample overlaps with that of the BCGs it is dominated by early–type galaxies.

A 'non-BCG cluster galaxy' sample is also constructed. This consists of those galaxies within the 'all galaxy' sample which are within $3r_{200}$ and $3\sigma_{\rm v}$ of one of the 625 clusters identified by von der Linden et al., but which are not identified as a BCG.

For all galaxies, the rest-frame luminosities were calculated from the re-calibrated photometry using the KCORRECT algorithm (Blanton et al. 2003), which determines the best composite fit to the observed galaxy fluxes of a large number of template stellar population spectra, including three alternative models for dust extinction. Following Blanton & Roweis (2007), this same algorithm was used to derive stellar mass estimates: as shown by those authors, the stellar masses derived agree to typically within 0.1 dex of those derived by other methods (e.g. those of Kauffmann et al. 2003a, using the z–band magnitude and a mass–to–light ratio determined by the strengths of the 4000Å break and the $H\delta$ absorption in the galaxy spectrum). Other physical properties of the galaxies, such as their emission line strengths, were taken from the MPA pipeline catalogues available at http://www.mpa-garching.mpg.de/SDSS/.

2.2 Identification of radio–loud AGN

Best et al. (2005) identified the radio–emitting galaxies within the main spectroscopic sample of the SDSS DR2, by cross–comparing these galaxies with the National Radio Astronomy Observatory (NRAO) Very Large Array (VLA) Sky Survey (NVSS; Condon et al. 1998) and the Faint Images of the Radio Sky at Twenty centimetres (FIRST) survey (Becker et al. 1995). The use of a combination of these two radio surveys allowed a radio sample to be derived which was both reasonably complete ($\approx 95\%$) and highly reliable ($\approx 99\%$). They then used the optical properties of the galaxies to separate the radio–loud AGN from the radio–detected star–forming galaxies. This work has now been extended to include the DR4 data (Best et al. in prep), and these results were used to determine which galaxies from the SDSS spectroscopic samples are radio–loud AGN.

For the 141 brightest cluster galaxies with only photometric data, the same cross–comparison of the galaxy locations with the NVSS and FIRST radio surveys was repeated in order to determine which had associated radio emission. However, the lack of spectroscopic data for these galaxies meant that the previous method of distinguishing radio–loud AGN from star–forming galaxies could not be used. Instead, for the 37 photometric BCGs with radio detections, the classification was based solely upon the radio luminosity. Figure 1 shows the distribution of radio luminosities for the BCGs with spectroscopic data, split by their classification as either radio–loud AGN or radio–detected star–forming galaxies. Above $L_{1.4\rm GHz} = 10^{22.5}\rm W\,Hz^{-1}$ all but one radio detected BCGs are AGN, whereas below that

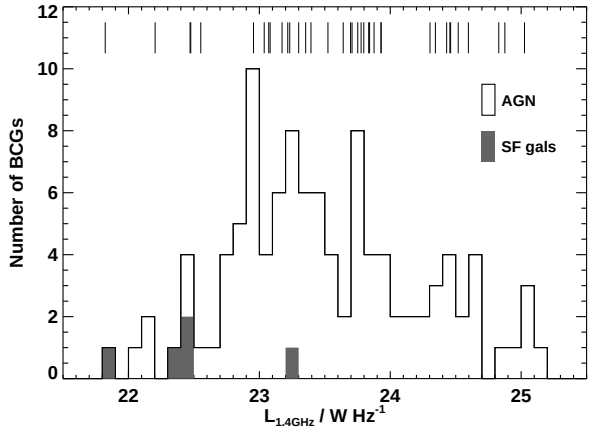

Figure 1. The histogram shows the distribution of radio luminosities of the radio–detected BCGs with SDSS spectroscopic data, split by their classification as either radio–loud AGN (unshaded) or radio–detected star–forming galaxies (shaded). The vertical lines at the top of the plot show the radio luminosities of the BCGs with only photometric data.

luminosity nearly half are star forming galaxies. The vertical lines at the top of the plot indicate the radio luminosities of the BCGs without spectroscopic data. The 32 photometric BCGs with $L_{1.4\rm GHz} > 10^{22.9}\rm W\,Hz^{-1}$ are almost certainly radio–loud AGN, and henceforth are classified as such. The other 5 all have radio luminosities below $10^{22.6}\rm W\,Hz^{-1}$ and are likely to include a mixture; their classification is less critical because most analyses are limited to only the BCGs brighter than $10^{23}\rm W\,Hz^{-1}$, but conservatively it is assumed that these are all star forming galaxies. It should be emphasised that the number of BCGs for which the origin of the radio emission is ambiguous is far too small for any misclassification to influence the results of the paper.

3 THE RADIO ACTIVITY OF BRIGHTEST CLUSTER GALAXIES

Using the radio sources defined from the SDSS DR2 catalogue, Best et al. (2005) showed that the probability of a galaxy to be a radio–loud AGN was dependent primarily upon its mass, determined either as the stellar mass ($f_{\rm radio-loud} \propto M_*^{2.5}$), or the black hole mass ($f_{\rm radio-loud} \propto M_{\rm BH}^{1.6}$). As discussed by Best et al. (2005), the difference between the slopes of these two relations arises mainly because of the increasing fraction of disk–dominated galaxies, with small black holes, at stellar masses $M_* \lesssim 10^{11} M_\odot$. These host fewer radio–loud AGN, and thus decrease the radio–loud fraction at low stellar masses, leading to a steeper dependence on stellar mass.

Figure 2 shows the percentage of brightest cluster galaxies that are radio–loud AGN, as a function of stellar mass. For comparison, the equivalent relation is also shown for the all galaxy sample. The brightest cluster galaxies are clearly offset from the 'all galaxy' relation, and their relation shows a different slope[1]: the fraction of BCGs that

[1] It should be stressed that the same conclusions are reached if

is radio–loud increases roughly as $M_*^{1.0}$ and is an order of magnitude higher than that of all galaxies for stellar masses below $10^{11}M_\odot$, but comparable to that of all galaxies at stellar masses above $5\times10^{11}M_\odot$. The increasing similarity of the two radio-loud fractions with increasing mass is actually not surprising, since at masses above $10^{11.5}M_\odot$ around a third of the 'all galaxy' population are classified as BCGs, and many of the remainder may be BCGs missed by the current sample. Note that from these data it is not possible to tell whether the increase in the radio–loud fraction of BCGs, relative to that of other galaxies, is due to radio–AGN activity being triggered more frequently in BCGs, or the BCG radio sources being longer lived (e.g. because the higher pressure environment of the dense cluster environment slows down the source expansion).

Black hole mass may be considered to be a more fundamental parameter than stellar mass when considering nuclear activity, and Best et al. (2005) estimated this for the SDSS DR2 galaxies using the velocity dispersion versus black hole mass relation of Tremaine et al. (2002): $\log(M_{\rm BH}/M_\odot) = 8.13 + 4.02\log(\sigma_*/200{\rm km\,s^{-1}})$. However, there is some doubt as to whether this 'normal galaxy' relation is also applicable for BCGs, or whether these follow a different relation (e.g. von der Linden et al. 2006). In addition, velocity dispersion measurements are only available for those BCGs with spectroscopic observations. In order to avoid any potential biases therefore, and also to increase the sample size, in this paper the analysis is presented only as a function of stellar mass. As a check, relations were constructed as a function of black hole mass, assuming the velocity dispersion to black hole mass conversion to be the same as for normal galaxies; these are in broad agreement with those presented here for stellar mass.

Figure 3 compares the radio–loud fraction versus stellar mass relation for BCGs in rich versus poor clusters. The probability for a BCG of given stellar mass to host a radio–loud AGN is independent of the velocity dispersion of the surrounding cluster. Because BCGs in the richest clusters tend to be more massive than those in poorer clusters, the fraction of BCGs which host radio–loud AGN still turns out to be higher in more massive clusters (marginally at least; $21\pm2\%$ in the $\sigma_{\rm v} > 500{\rm km\,s^{-1}}$ clusters in this sample, compared to $17\pm2\%$ for those with $\sigma_{\rm v} < 500{\rm km\,s^{-1}}$), but it is the mass of the BCG, rather than the properties of its surroundings, which controls the likelihood of it being radio–loud.

Best et al. (2005) also found that for 'all galaxies' the distribution of radio luminosities of the radio–loud AGN was independent of the mass of the host galaxy. This result is shown in the top panel of Figure 4 for three different mass ranges. Also shown on the same plot are the distributions of radio luminosities for brightest cluster galaxies in the same mass ranges. The shape of the radio luminosity function does not change significantly either as a function of mass for brightest cluster galaxies, or between the brightest cluster galaxy and all galaxy samples[2]: only the normalisation of the radio luminosity function changes. The bottom panel of Figure 4 compares the distribution of radio luminosities of BCGs in rich and poor clusters: again, these are broadly in agreement, although there is tentative evidence that there

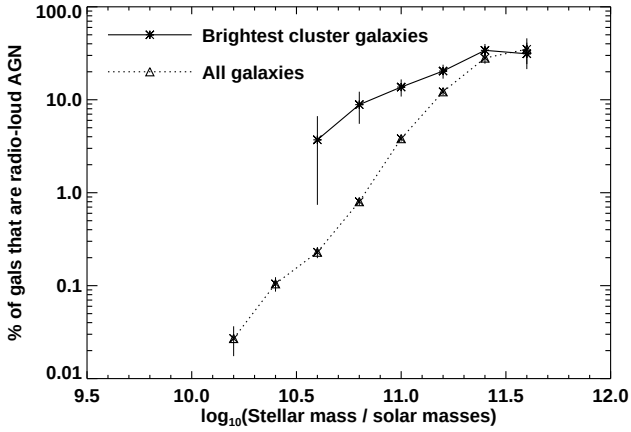

Figure 2. The percentage of galaxies that are radio–loud AGN, as a function of stellar mass, for 'all galaxies' and for 'brightest cluster galaxies'. Brightest cluster galaxies are more likely to be radio–loud than other galaxies of the same stellar mass, and the two relations have different slopes.

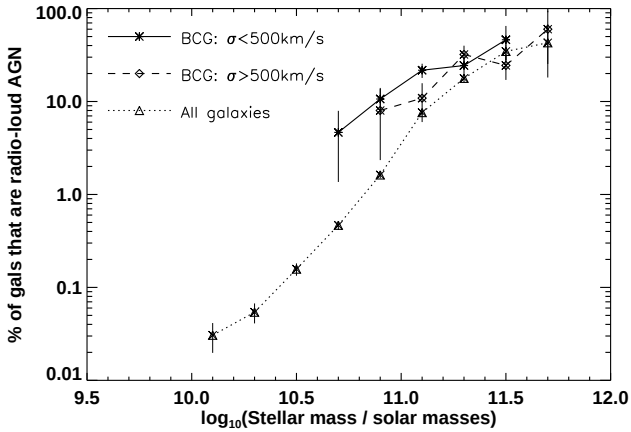

Figure 3. The percentage of brightest cluster galaxies that are radio–loud AGN, as a function of stellar mass, split by the velocity dispersion of the clusters. At given stellar mass, the radio–loud fraction of BCGs is indistinguishable between rich and poor clusters.

the plots are made as a function of galaxy luminosity, instead of stellar mass, as demonstrated in von der Linden et al. (2006). Similarly, if the 'all galaxy' sample is restricted to just those classified as early-type galaxies by using their SDSS morphological parameters concentration index and surface mass density (cf. Kauffmann et al. 2003b, and discussion therein) then the results are also largely unchanged at masses above $5\times10^{10}M_\odot$, where it overlaps with the BCG sample. This is because the galaxies at high stellar masses are dominated by old ellipticals, whose mass-to-light ratios do not vary strongly.

[2] The only variation in shape is a flattening at low radio luminosities, of both BCGs and all galaxies, when the radio–loud fraction exceeds $20-30\%$; as Best et al. (2005) argued, such flattening must occur at some point, since the radio–loud fraction cannot exceed 100%.

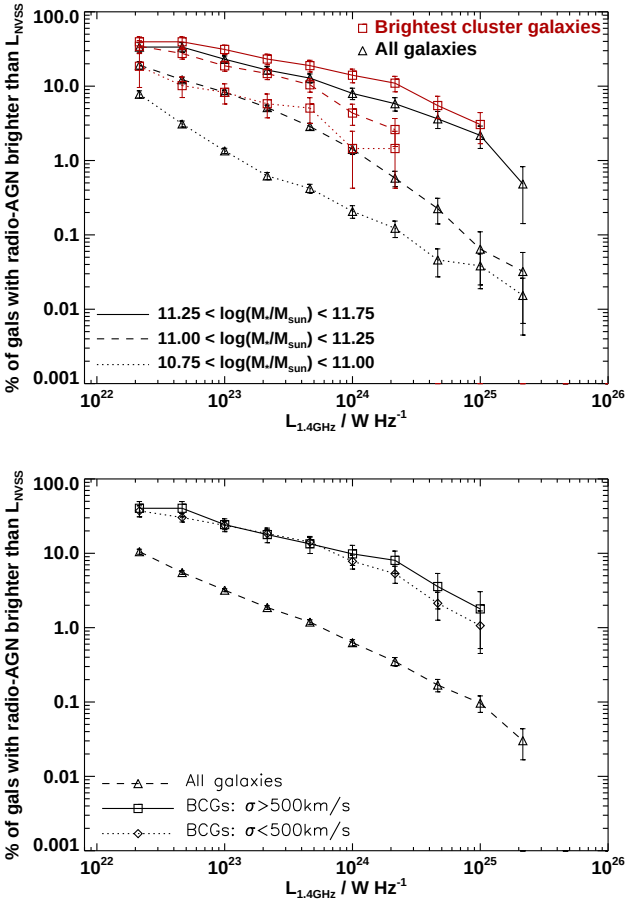

Figure 4. *Top:* The percentage of galaxies which are radio–loud AGN brighter than a given radio luminosity, for 'all galaxies' (black lines) and the subsample of 'brightest cluster galaxies' (red lines) in three different ranges of stellar mass. There is no evidence for any significant difference in the shape of the luminosity functions, either as a function of stellar mass, or between brightest cluster galaxies and all galaxies: only the normalisation of the relation changes. *Bottom:* The distribution of radio luminosities of BCGs split by the velocity dispersion of their host clusters, for BCGs with masses in the range $10^{11} < M_*/M_\odot < 5 \times 10^{11}$, compared to that of normal galaxies.

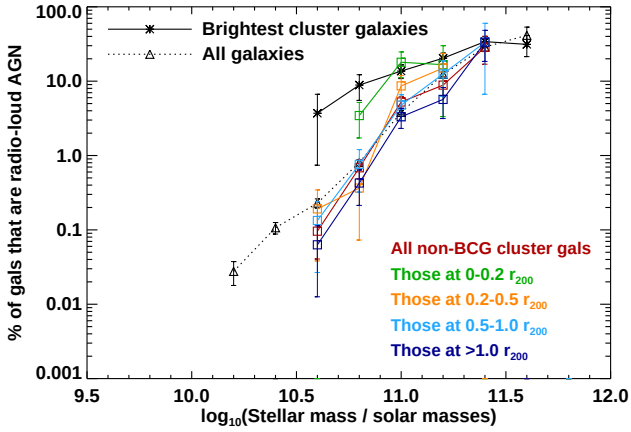

Figure 5. The percentage of galaxies that are radio–loud AGN, as a function of stellar mass, for 'non–BCG cluster galaxies' (red line) as compared to the 'all galaxy' (dotted black line) and 'brightest cluster galaxy' (solid black line) samples. The other coloured lines indicate the radio–loud AGN fractions for subsets of the non–BCG cluster galaxies within different ranges of projected cluster-centric radii: the green, orange and cyan lines show the relations for galaxies with redshifts within $2\sigma_v$ of the mean cluster redshift and with projected radii of 0–0.2r_{200}, 0.2–0.5r_{200} and 0.5–1.0r_{200} respectively, while the dark blue line shows the equivalent relation for cluster galaxies outwith 1.0r_{200}.

may be more high luminosity radio sources in richer clusters. A larger sample will be required to confirm this result.

4 RADIO–LOUD AGN ACTIVITY IN OTHER CLUSTER GALAXIES

Many authors have examined the environments of radio–loud AGN (e.g. Prestage & Peacock 1988; Hill & Lilly 1991; Miller et al. 2002; Best 2004) and have found that these sources appear to favour galaxy group and weak cluster environments. Nevertheless, Ledlow & Owen (1996) demonstrated that the bivariate radio–optical luminosity function of cluster galaxies is very similar to that of field galaxies. This indicates that the preference for radio sources to be located in dense environments may simply be due to the concentration of massive galaxies within clusters, coupled with the strong mass dependence of the radio–loud fraction. The SDSS data and the C4 cluster sample allow this issue to be investigated in more detail.

Figure 5 shows the fraction of non–BCG cluster galaxies (red line) that are radio–loud AGN, as a function of stellar mass, in comparison to all galaxies and to brightest cluster galaxies. The radio–loud AGN fraction of cluster galaxies matches that of all galaxies at all stellar masses (except possibly the lowest mass bin, where it might be slightly lower). Figure 6 similarly shows that the distribution of radio luminosities of the cluster galaxies is the same as that of non-cluster galaxies. Overall, then, for galaxies of given stellar mass the radio luminosity functions are the same inside and outside of clusters, as was found by Ledlow & Owen (1996). They are also independent of the velocity dispersion of the host cluster, as shown in Figure 7.

Figures 5 and 6 also show the radio–loud AGN fraction and radio luminosity distribution for various subsets of cluster galaxies in different ranges of projected radius from the cluster centre. It is striking that galaxies with redshifts within $2\sigma_v$ of the mean cluster redshift and $0.2r_{200}$ of the cluster centre have an enhanced probability of being radio–loud AGN, approaching that of the BCGs, although once again with the same distribution of radio luminosities. Outside of $0.2r_{200}$ there is no substantial change in the radio–loud fraction with radius (there may be a marginal fall with increasing radius, but this is within the errors, and insignificant compared to the increase within $0.2r_{200}$).

One concern is that the increase in the radio–loud fraction of galaxies near the centre of the cluster may arise as a result of mis-identification of some BCGs. The evidence suggests, however, that this is not the case. There are 13 clusters where a radio source is associated with a non–BCG cluster galaxy within $0.2r_{200}$. Of these, the identified BCG

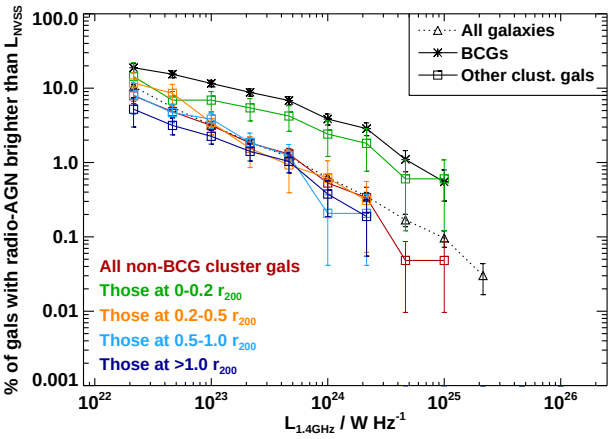

Figure 6. The percentage of galaxies which are radio–loud AGN brighter than a given radio luminosity for 'non–BCG cluster galaxies' (red line) as compared to the 'all galaxy' (dotted black line) and 'brightest cluster galaxy' (solid black line) samples. These plots are constructed considering all galaxies in the $10^{11} < M_*/M_\odot < 10^{12}$ mass range, but then scaling the BCG line uniformly down by a factor of 1.7 to account for the higher median mass of BCGs within this mass range (the median masses of galaxies in all other subsamples are statistically indistinguishable). The other coloured lines indicate the equivalent relations for different subsets of the non–BCG cluster galaxies with different projected radii, as defined in Figure 5. The radio–loud AGN fraction is boosted for galaxies within $0.2r_{200}$ of the cluster centre, but retains the same overall shape.

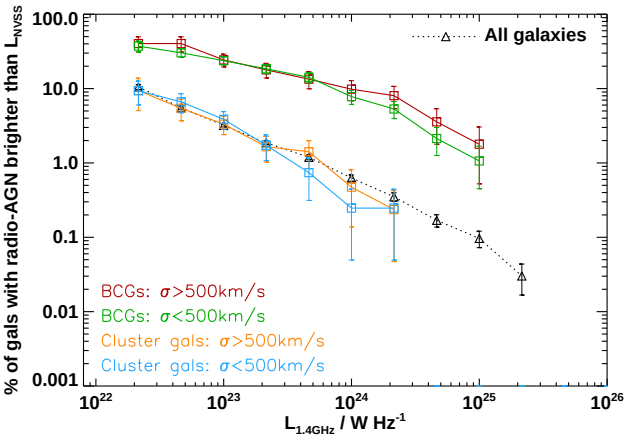

Figure 7. The distribution of radio luminosities of non–BCG cluster galaxies, split by the velocity dispersion of their host clusters, as compared to all galaxies and to brightest cluster galaxies. Only galaxies with masses in the range $10^{11} < M_*/M_\odot < 5\times10^{11}$ are included on the plot.

is also radio–loud in 6 ($\equiv 46\pm19\%$) of the clusters: this fraction is comparable to (or even above) that of other BCGs of the same mass ($\approx 10^{11.3} M_\odot$), and far above that of non–BCG cluster galaxies. Further, of the 7 clusters with a radio–loud galaxy within $0.2r_{200}$ but a radio–quiet BCG, visual analysis indicates that the BCG identification is absolutely unambiguous in 5 of the cases, and should be reliable in the other two. Finally, the distribution of ratios of radio galaxy mass to BCG mass is indistinguishable between the 13 $r < 0.2r_{200}$ radio galaxies and the radio galaxies at larger radii, in contrast to what would be expected if these were misidentified BCGs. In conclusion, therefore, the enhanced radio–loud fraction for galaxies within $0.2r_{200}$ of the cluster centre appears to be a genuine physical effect.

5 EMISSION–LINE AGN ACTIVITY IN CLUSTER GALAXIES

It is interesting to compare the enhanced radio–loud AGN activity of brightest cluster galaxies and other galaxies in the central $0.2r_{200}$ of the cluster, with their emission line properties. Kauffmann et al. (2003c) identified emission–line galaxies in the SDSS spectroscopic sample, and used the [OIII] 5007 / Hβ versus [NII] 6583 / Hα emission line ratio diagnostic diagram (Baldwin et al. 1981) to separate out galaxies with AGN activity from those galaxies where the emission lines are associated with star formation[3]. The fraction of galaxies hosting emission line AGN rises shallowly up to $10^{10.5} M_\odot$, and is then flat at higher masses, which is substantially different from the very steep mass dependence of the radio–loud AGN fraction (Best et al. 2005). This result is shown in Figure 8 for the 'all galaxy' sample (for AGN defined in the same way as Kauffmann et al. 2003c, and with $L_{[\rm OIII]5007} \gtrsim 10^{6.5} L_\odot$) and is compared to the fraction of galaxies hosting emission–line AGN for the brightest cluster galaxy and non-BCG cluster galaxy samples. Also shown are the relations for subsamples of cluster galaxies at different cluster-centric radii. Note that once again, making this plot as a function of galaxy luminosity instead of mass leads to essentially the same results.

Brightest cluster galaxies are found to be less likely to possess emission–line AGN activity than 'all galaxies' of the same stellar mass, by a factor of 2–3 at all masses. This suppression of emission–line AGN activity is also true of other cluster galaxies: cluster galaxies as a whole are found to be about 20% less likely to show emission–line AGN activity than all galaxies, consistent with the results of previous studies (e.g. Miller et al. 2003; Kauffmann et al. 2004). Splitting the cluster galaxies into subsamples at different radii demonstrates that the suppression gets progressively stronger as the cluster centre is approached: outside r_{200} the fraction of cluster galaxies displaying emission–line AGN activity matches that of 'all galaxies', but this drops by a factor of at least 2 for those galaxies within $0.3r_{200}$. Interestingly the BCGs show the same likelihood of emission line AGN activity as other galaxies of the same mass towards the centre of the cluster: unlike for the radio activity, the special location of BCGs does not appear to lead to different emission–line AGN activity.

This result may seem to be at variance with the luminous extended emission line structures known to exist around some BCGs (e.g. Heckman et al. 1989; Hatch et al. 2006, and references therein). Part of this difference may be

[3] It should be stressed that since the parent sample for that analysis, like the current one, was the SDSS 'main galaxy sample', the AGN selected are mostly type–II AGN. Powerful type-I quasars will be missed from the sample.

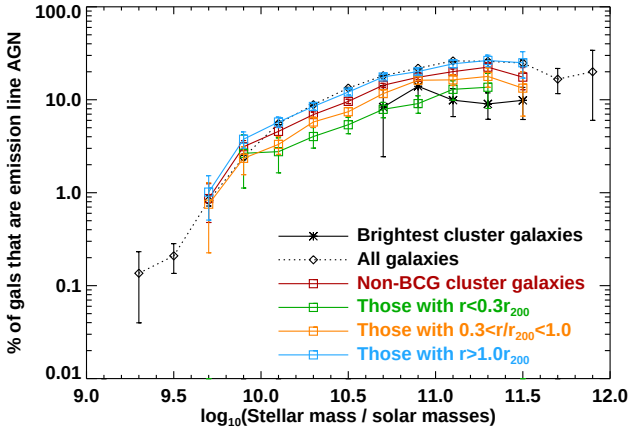

Figure 8. The percentage of galaxies that show emission–line AGN activity (with $L_{[OIII]5007} \gtrsim 10^{6.5} L_{\odot}$), as a function of stellar mass, for 'all galaxies' (dotted black line), 'brightest cluster galaxies' (solid black line) and 'non–BCG cluster galaxies' (red line). Also shown are equivalent relations for subsamples of cluster galaxies in different cluster-centric radial ranges. Emission line AGN activity is suppressed within r_{200} of the cluster centre, with the strength of the suppression increasing with decreasing radius.

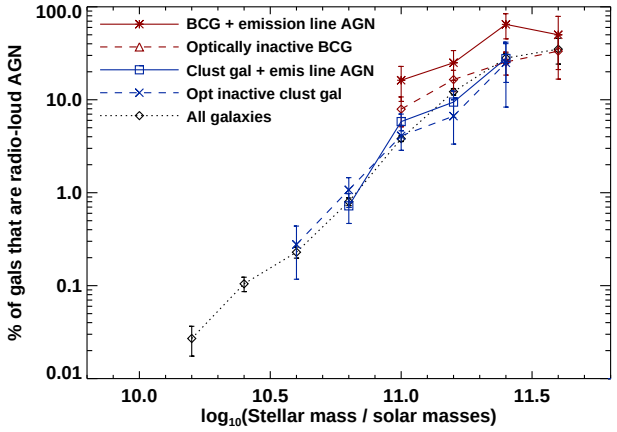

Figure 9. The percentage of brightest cluster galaxies which are also emission–line selected AGN (solid red line) and those which are optically–inactive (dashed red line), that are classified as radio–loud AGN, as a function of stellar mass. This is compared to the fraction of normal galaxies that are radio–loud AGN (black line; this is independent of whether or not they optical AGN), and with the equivalent relations for non-BCG cluster galaxies (blue lines).

because the SDSS fibre apertures are small ($\sim$ 5kpc diameter at $z \approx 0.1$), whilst the line emission seen in the above studies can extend for several tens of kiloparsec. More important, however, is a difference in the type of BCG studied. Edwards et al. (2007) recently studied the line emission from BCGs and found that the fraction of the BCG population as a whole that display emission lines is about 15%, and is comparable to that of other massive galaxies near the cluster centres. These results are in full agreement with those found here, shown in Figure 8. However, these authors also find that if they restrict analysis to just those BCGs which are within 50 kpc of the X–ray centre of a cooling flow cluster, then the fraction which display emission lines rises to $\sim$ 75%. It is such massive, strong cooling flow clusters that have been the main focus of the previous emission line studies, and the extended emission line activity detected is associated with the cooling flow. The current results and those of Edwards et al. demonstrate that more typical BCGs do not have enhanced emission line activity.

A further interesting test concerns the relationship between radio and optical emission line activity. Best et al. (2005) found that for 'all galaxies' the probability of a galaxy hosting a low luminosity radio source was independent of whether or not it was an emission–line AGN. Figure 9 investigates this for the brightest cluster galaxies and the non–BCG cluster galaxies. Unlike the situation for all galaxies, the radio–loud fraction for brightest cluster galaxies does depend upon the emission line properties: BCGs which show emission–line AGN activity are 2–3 times more likely at all masses to host radio–loud AGN than those which are optically inactive — although the latter still show a higher radio–loud fraction than non–BCG galaxies. Other cluster galaxies behave in the same way as 'all galaxies', with the radio–loud fraction being the same regardless of the optical properties.

6 IMPLICATIONS FOR THE ORIGIN OF LOW LUMINOSITY RADIO-LOUD AGN

The apparent independence of emission line and radio–loud AGN activity, coupled with the fundamentally different dependencies of their prevalences on galaxy mass, led Best et al. (2005) to conclude that low luminosity radio–loud AGN activity[4] and emission line AGN activity are distinct physical phenomenon. They argued that emission–line AGN activity tracks the accretion of cold material onto black holes through standard accretion disks, and thus reflects the major mode of growth of the black holes (see discussion in Heckman et al. 2004), whilst low luminosity radio sources represent re-triggering of pre–formed massive black holes in old elliptical galaxies. The accretion rates in these radio sources are comparably low, and the activity is reflected in the production of low power radio jets but relatively little emission at optical, ultraviolet and infrared wavelengths. Best et al. (2005) argued that the accreting material in the radio mode was hot gas, cooling out of the envelopes of elliptical galaxies. The results for the brightest cluster galaxies lend further credence to this scenario: since BCGs are located at the bottom of the cluster potential well, they are also the repository for cooling intracluster gas. This increased supply of hot gas naturally leads to the observed increased radio–loud AGN fraction.

Best et al. (2006) suggested that one possibility for the accretion mechanism is Bondi–Hoyle accretion from a strong cooling flow (see also the recent work of Allen et al. 2006); the accretion rate for this is given by Croton et al. (2006)

[4] The volume probed by the SDSS data is insufficient to investigate the rare, powerful, classical double (Fanaroff & Riley (1974) class 2, or FR II) radio sources, which do have associated optical AGN activity, but instead only investigate the distinct population of lower luminosity (mostly FR I) radio sources.

as $\dot{m}_{\rm Bondi} \approx G\mu m_p kTM_{\rm BH}/\Lambda$, where μm_p is the mean mass of particles in the gas, and Λ is the cooling function. For isothermal elliptical galaxy halos, $T \propto \sigma^2$; the black hole mass versus velocity dispersion relation (e.g. Tremaine et al. 2002) then implies $T \propto M_{\rm BH}^{0.5}$. Λ is relatively independent of temperature (and hence black hole mass) at the temperature of elliptical galaxy haloes, and therefore the Bondi accretion rate scales roughly as $M_{\rm BH}^{1.5}$, which is approximately the same exponent as the radio–loud AGN fraction for all galaxies. Interestingly, for BCGs the approximation $T \propto M_{\rm BH}^{0.5}$ is not valid, because the temperature of the gas accreting on to the BCG is not directly related to the properties of the host galaxy, but rather is controlled by the larger–scale environment. In a cluster of given temperature, therefore, the Bondi–Hoyle accretion rate might be expected to scale linearly with the black hole mass (and hence stellar mass) of the BCG, which is exactly what is observed in Figure 2.

One surprising result is that there is no increase in the radio–loud AGN fraction in higher velocity dispersion (mass) clusters: these would be expected to have higher cooling rates, raising the radio–loud fraction. For the Bondi–Hoyle mechanism, at fixed black hole mass the accretion rate scales as T/Λ, and at the temperature of clusters, Λ increases approximately as $T^{0.5}$. The accretion rate therefore scales as $T^{0.5}$, and thus roughly linearly with the cluster velocity dispersion, σ_v. This would predict nearly a factor of two difference between the accretion rates, and hence the radio-loud AGN fractions, of the clusters in the low and high velocity dispersion bins, which ought to be (just) detectable from the current data. The failure to observe this effect may be because the relevant temperature is that of the gas in the central regions of the cluster, and most massive clusters have cooler cores associated with the cooling flow; this reduces the expected difference in accretion rate between high and low mass clusters, possibly to within the errors of the current measurements. Investigating this with a much larger sample of clusters, or using clusters for which the core temperatures of the X–ray gas have been measured, would provide a critical test of this model.

The increased likelihood of radio–loud AGN activity for non–BCG galaxies within $0.2r_{200}$, particularly the more massive ones, suggests that the accretion of gas onto these galaxies is also controlled to some extent by the intracluster medium. It is intriguing that the cooling radius of clusters (that is, the radius within which the cooling time is less than the Hubble time) is typically about 10% of r_{200}: thus, the intracluster medium affects the radio–loud fraction of only those galaxies within, or close to, the cooling radius.

The emission–line properties of the BCGs provide further support for the interpretation that different accreting material is responsible for low–luminosity radio–loud AGN activity than that for emission line AGN activity. In contrast to the radio–loud AGN activity, the emission–line properties of BCGs are in general suppressed relative to galaxies outside clusters, and are comparable to those of other galaxies of the same mass in the inner regions of the clusters. This implies that there is a lack of cold gas to fuel the black holes in these galaxies. This result is undoubtedly related to the decreased levels of star formation activity in cluster environments (e.g. Lewis et al. 2002; Gómez et al. 2003; Mateus & Sodré 2004, and references therein).

Interestingly, those BCGs which do show emission–line activity also show an enhanced level of radio–loud AGN activity, suggesting that in BCGs (in contrast to other galaxies) there may be some connection between the processes which drive the radio and emission–line activity. This is consistent with the discussion in Section 5 that the BCGs of cooling flow clusters frequently have associated extended emission–line nebulae. The properties of these are similar to those of low–ionisation nuclear emission–line regions (LINERs; e.g. Voit & Donahue 1997), and so may be mistaken for AGN activity. Thus, the emission lines detected in some BCGs may not actually arise from AGN activity, but rather from the cluster–scale cooling flow which fuels the radio–loud AGN activity. Figure 10 shows the location of the SDSS emission–line BCGs on the traditional 'BPT' (Baldwin et al. 1981) emission line diagnostic diagram. As a guide, this diagram has been divided into regions (as defined by Kauffmann et al. 2003c) indicating the expected locations of star forming galaxies, Seyferts, LINERs, and galaxies whose spectrum is a star formation – AGN composite. The majority of the emission–line BCGs, especially those which are radio–loud AGN, are found in the LINER region of the diagram, and so some of this line emission may indeed be directly associated with the cooling flows.

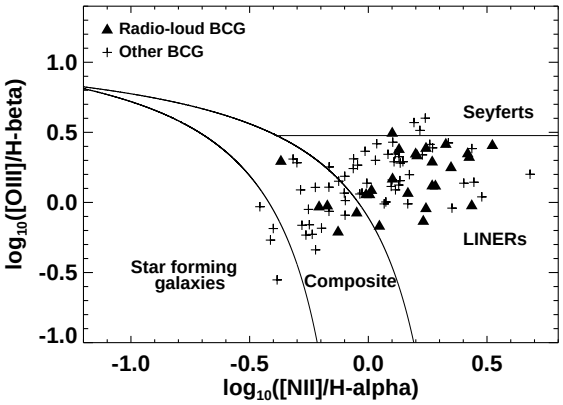

Figure 10. An emission line diagnostic plot for the brightest cluster galaxies with emission lines, divided into different classifications for the source of ionisation of the emission lines following Kauffmann et al. (2003c). The majority of these BCGs, especially the radio-loud ones, have LINER-like emission line spectra.

7 RADIO–LOUD AGN HEATING OF COOLING FLOWS

7.1 The mass–dependent heating rate of BCGs

Radio–loud AGN have relatively short lifetimes ($10^7 - 10^8$ years), and so the very high fraction of galaxies which host radio–loud AGN (over 30% at the highest masses) implies that this activity must be constantly re–triggered. The probability of a galaxy of a given mass hosting a radio source of given radio luminosity (cf. Figure 4) can therefore be interpreted, probabilistically, as the fraction of its time that a galaxy of a given mass spends as a radio source of given luminosity. Monochromatic radio luminosity represents only a tiny fraction of the energetic output of a radio source, how-

ever, with the mechanical energy of the radio jets being 2–3 orders of magnitude larger. In order to determine the time–averaged heating output of radio–loud AGN, therefore, it is necessary to derive a conversion between the radio luminosity and mechanical luminosity of the radio sources.

Any such conversion is necessarily approximate because the precise ratio between mechanical and radio luminosities is both unknown, and varies throughout the lifetime of a radio source. Nevertheless, it is reasonable to assume that there may be some statistical average relationship (e.g. averaging over all ages of a radio outburst), such that a conversion between the radio and mechanical luminosity functions can still be carried out at a population level. Such a conversion should be largely independent of the host galaxy mass (indeed, if it were not, then the similarity of the radio luminosity shapes for galaxies of different masses would be a remarkable co-incidence). The mean conversion relation can be determined empirically using data from the observed bubbles and cavities produced by radio sources in the intracluster medium of groups and clusters of galaxies. Bîrzan et al. (2004) compiled data for the energies, ages and radio luminosities of these cavities, and Best et al. (2006) used these data to determine that:

$$\frac{L_{\rm mech}}{10^{36}{\rm W}} = (3.0 \pm 0.2) \left(\frac{L_{1.4{\rm GHz}}}{10^{25}{\rm W Hz^{-1}}} \right)^{0.40 \pm 0.13}. \quad (1)$$

Given the result of Section 3 that the *shape* of the radio luminosity function is the same between galaxies of all masses, then converting the radio luminosity function to a mechanical luminosity function using Equation 1 means that the shape of the mechanical luminosity function is also similar for galaxies of different masses (and for BCGs). Integrating across this, Best et al. estimated the time–averaged AGN heating output of all galaxies, as a function of black hole mass[5]:

$$\bar{H}_{\rm all} = 1.6 \times 10^{34} (M_{\rm BH}/10^8 M_\odot)^{1.6} {\rm W}. \quad (2)$$

In this equation, the black hole mass dependence arises from directly from the scaling of the radio-loud fraction with black hole mass (ie. that more massive black holes are switched on for a larger fraction of the time). Errors in the conversion of radio to mechanical luminosity, and other such uncertainties, only affect the normalisation factor. This can be accounted for by introducing a factor f into Equation 2, giving:

$$\bar{H}_{\rm all} = 1.6 \times 10^{34} f (M_{\rm BH}/10^8 M_\odot)^{1.6} {\rm W}. \quad (3)$$

The factor f accounts for a range of possible uncertainties, and these are discussed in detail in Section 7.2. It is likely, however, that it has a value reasonably close to unity. It is noteworthy that Best et al. (2006) found that a value $f \approx 1$ was appropriate for heating to balance radiative cooling losses in elliptical galaxies.

The method described above can also be applied to the brightest cluster galaxies. Taking the result from Section 3 that the radio luminosity function of BCGs has the same shape as that of 'all galaxies'[6] and that only the normalisation differs, then integrating the distributions in Figure 4, and incorporating the same factor f gives:

$$\bar{H}_{\rm BCG} = 2.3 \times 10^{35} f (M_*/10^{11} M_\odot) {\rm W}. \quad (4)$$

As shown in Section 4, the time averaged heating rate of the non–BCG cluster galaxies outwith $0.2r_{200}$ is the same as that for 'all galaxies', given in Equation 3. For the cluster galaxies within $0.2r_{200}$, the boosted radio–loud AGN fraction will produce a heating rate between that of the BCGs and that of all galaxies, but the sample is too small to accurately determine this. For the analysis in the following sections, the limiting cases of $\bar{H}_{\rm all}$ and $\bar{H}_{\rm BCG}$ were both considered for these galaxies, and it was found that there was negligible difference between the results produced.

7.2 The uncertainty factor f

The analysis method adopted here assumes that a good mean conversion can be made between radio and mechanical luminosity. There are, however, examples of cluster radio sources (e.g., MS0735.6+7421, Abell 1835; McNamara et al. 2005; McNamara et al. 2006) where the mechanical power estimate is 2–3 orders of magnitude higher than that estimated by Equation 4. Bîrzan et al. (2004) and Rafferty et al. (2006) showed that the mechanical luminosity also relates strongly to the X-ray luminosity of the system, suggesting that a full understanding of these systems will require consideration of more parameters than simply the radio luminosity. Nevertheless, the uncertainty factor f in Equations 3 and 4, can be used to broadly encompass these additional effects. It is therefore worthwhile considering in detail what uncertainties are contained within the factor f, as this has important consequences for the interpretation of the results. The uncertainty can be categorised in three parts.

(i) *Uncertainty in the estimates of cavity mechanical luminosities.* The calculations of Bîrzan et al. have significant uncertainties in the estimates of both the energies and the ages of the radio source cavities. In addition, Bîrzan et al. calculate the pV energy of the cavity, but the enthalpy of the cavity is given by $\frac{\gamma}{\gamma-1}$pV, which is 4pV for the relativistic plasma of the radio lobes. There may also be additional heating directly from the radio jets: Nusser et al. (2006) argue that the mechanical energy may exceed pV by a factor of 10.

(ii) *Uncertainty in the radio to mechanical luminosity conversion.* As discussed above, the varying radio luminosity during a source lifetime means that this conversion is only accurate in an average sense over the whole radio source population; however, to first order it ought to be both reasonable, and largely independent of host galaxy mass. There have been arguments that this conversion might be dependent upon environment, however: for fixed jet kinetic power,

[5] It is worth noting that Nipoti & Binney (2005) adopt a similar method but with the opposite approach: beginning from the assumption that AGN mechanical heating balances cooling, they use the Bîrzan et al. (2004) results to derive a radio luminosity function for radio–loud AGN, which they show to be in good agreement with that observed.

[6] Note that if the radio luminosity function for BCGs shows a weaker break (which would be consistent with the observations for clusters with $\sigma_{\rm v} > 500{\rm km\,s^{-1}}$) then the derived heating rate would be higher — but even if there was no break at all out to an extreme luminosity of $10^{30}{\rm W\,Hz^{-1}}$ the increase would only be a factor of 1.7.

radio luminosities could be higher in clusters, due to the confining effect of the dense intracluster medium reducing adiabatic expansion losses in the radio lobes and therefore increasing the radio synchrotron emission (e.g. Barthel & Arnaud 1996, and references therein). If correct, this would lead to slightly lower values of f in denser systems. Alternatively, as suggested by systems such as MS0735.6+7421 and Abell 1835 discussed above, individual outbursts with extreme mechanical to radio luminosity ratios may become more important in clusters, effectively raising the value of f.

(iii) *Uncertainty in how much of the cavity mechanical energy gets converted to heat within the cooling radius.* The heating rate calculations above assume that all of the mechanical energy of the cavities is used to heat the intracluster medium, and that such heating occurs within the cooling radius of the cluster. If either the radio source energy is not efficiently converted to heat (e.g. because of inefficient production of sound/shock waves), or much of that heating occurs beyond the cooling radius of the cluster, then this could lead to values of $f \ll 1$.

7.3 The importance of the BCG in radio–mode heating

The top panel of Figure 11 shows the ratio of the time-averaged radio–mode heating rate, summed across all non-BCG cluster galaxies[7], to that of the BCG, for all of the 625 SDSS clusters. These are calculated using Equations 3 and 4, assuming that the same value of f is appropriate for both. In most groups and low mass clusters the heating is dominated by the BCG alone, but for the richer clusters, the sum total of other galaxies can provide significantly more heating than the BCG alone. This heating from the non–BCG galaxies is, however, spread over a volume very much larger than the cooling radius of the cluster.

Peres et al. (1998) have determined the cooling radii of an X–ray flux limited sample of 55 nearby clusters, and these cooling radii (converted to the cosmology adopted here) are plotted as a function of cluster velocity dispersion in the upper panel of Figure 12. As most of these clusters are of high velocity dispersion, these data have been supplemented by three lower velocity dispersion groups for which cooling radii have also been measured: NGC1550 (Sun et al. 2003), RGH80 (Xue et al. 2004) and NGC6482 (Khosroshahi et al. 2004). The solid line shows a linear fit (in log space) to the data, calculated using the EM and Buckley–James linear regression techniques for censored data, within the ASURV survival analysis package (LaValley et al. 1992): $r_{\rm cool} = 67(\sigma_v/500{\rm km\,s^{-1}})^{0.45}{\rm kpc}$. Using this fit to estimate the cooling radius of each SDSS cluster, the lower panel of Figure 11 shows the ratio of radio–mode heating from non–BCG cluster galaxies projected within the cooling radius to

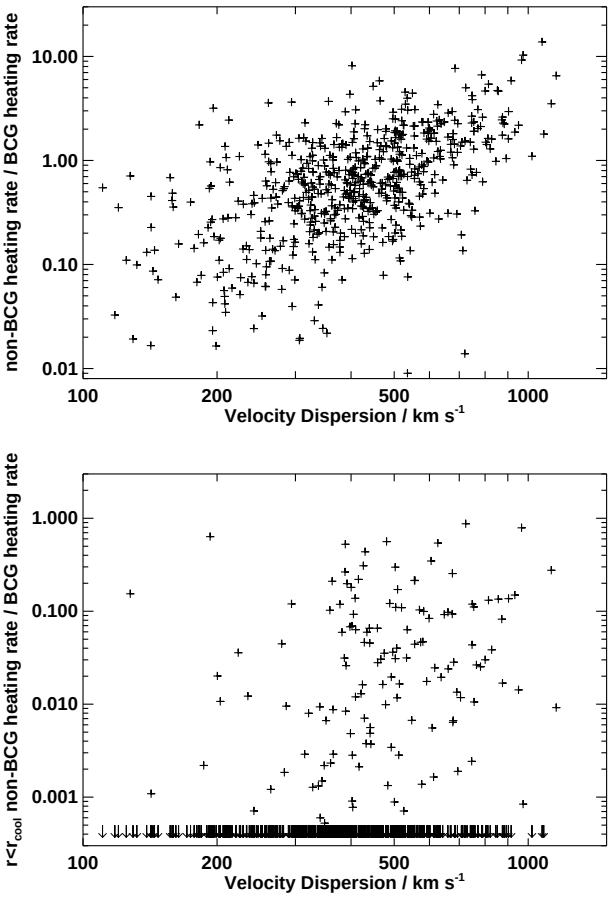

Figure 11. *Top:* the ratio of the time–averaged radio–mode heating rate of all non–BCG cluster galaxies, to that of the BCG, as a function of velocity dispersion, for the 625 SDSS clusters. *Bottom:* the same plot, but restricted to only those non–BCG cluster galaxies which are projected to lie within the cooling radius of the cluster.

that of the BCG. This analysis demonstrates that only the BCG is really relevant when calculating radio–mode heating within the cooling radius: unless there are other effects not considered here (e.g. the efficiency factor f varies between BCGs and non-BCGs for some unknown reason) then the model of Nusser et al. (2006) whereby cooling flows are suppressed by the combined activity of all cluster galaxies does not seem to work. This is a result of the very strong mass dependence of the radio–loud AGN fraction (with BCGs being the highest mass galaxies) coupled with the additional boosting of the radio–loud fraction amongst the BCG population.

7.4 AGN heating versus cooling in clusters

Figure 13 shows the time–averaged mechanical luminosity associated with radio–loud AGN, assuming $f = 1$, summed across all cluster galaxies, as a function of cluster velocity dispersion. For comparison, four recently derived relations between bolometric X–ray luminosity and velocity dispersion are also shown (Xue & Wu 2000; Mahdavi & Geller 2001; Ortiz-Gil et al. 2004; Popesso et al. 2005). The com-

[7] Although the SDSS data only include the more luminous cluster galaxies, the very strong mass dependence of the radio–loud fraction means that the missing fainter galaxies should have a negligible contribution to the radio AGN heating rate. The SDSS data will also miss some of the brighter non–BCG cluster galaxies, for example due to fibre collisions, but the number of these will be small.

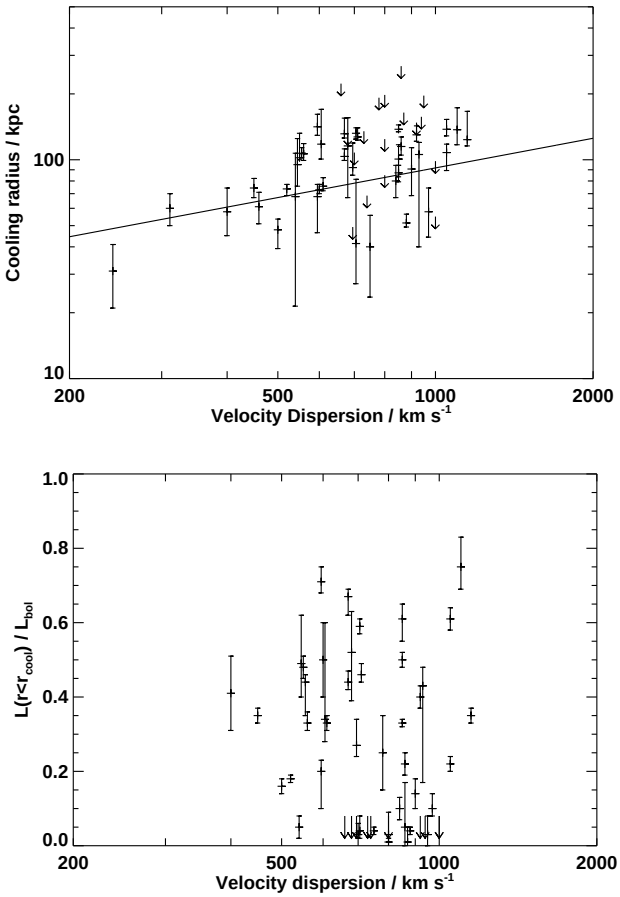

Figure 12. *Top:* the observed cooling radii of clusters and groups of galaxies, taken from Peres et al. (1998), Sun et al. (2003), Xue et al. (2004) and Khosroshahi et al. (2004), as a function of cluster velocity dispersion. The solid line represents a fit to the data using survival analysis techniques to properly account for the censored data. *Bottom:* the fraction of the X–ray luminosity of those clusters that arises from within the cooling radius, as calculated by Peres et al. (1998).

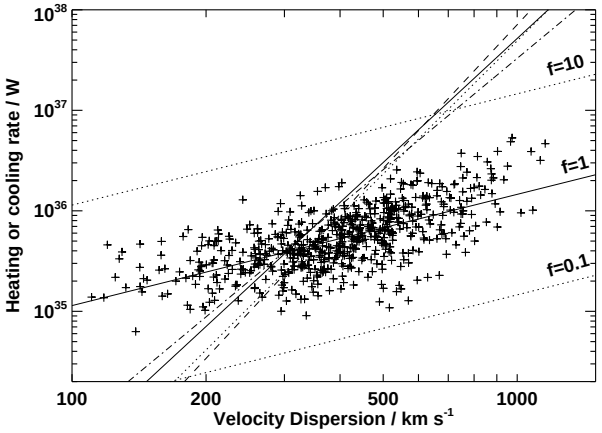

Figure 13. The data points show the time–averaged heating rate associated with radio–loud AGN activity, assuming $f = 1$ in Equations 3 and 4, summed across all galaxies in the clusters, as a function of cluster velocity dispersion. The solid line through these points, labelled '$f = 1$', is a straight-line fit to these points. The two dotted lines parallel to this represent scaled versions of this fit, showing where the data points would be located if $f = 0.1$ or $f = 10$. The remaining 4 lines indicate observed relations between bolometric X–ray luminosity and velocity dispersion for cluster and groups: solid line — Ortiz-Gil et al. (2004); dotted line — Mahdavi & Geller (2001); dashed line — Xue & Wu (2000); dash–dot line — Popesso et al. (2005).

bined heating rate of all radio–loud AGN increases much more slowly with cluster velocity dispersion than the σ^4 dependence of the radiative cooling rate. It is clear that (for $f = 1$) radio–loud AGN heating falls short of balancing the radiated X–ray luminosity for essentially all clusters and groups with $\sigma_{\rm v} \gtrsim 300{\rm km\,s^{-1}}$, and by an order of magnitude at the high mass end. However, much of the X–ray luminosity of the clusters arises from radii larger than the cooling radius, and does not need to be balanced by heating in order to avoid catastrophic cooling collapse. It is instructive, therefore, to calculate what fraction of the X-ray luminosity within the cooling radius the BCG radio–mode heating is able to balance.

Peres et al. (1998) determined the fraction of the total X–ray luminosity that is emitted from within the cooling radius for their sample of 55 clusters. These fractions are plotted as a function of velocity dispersion in the lower panel of Figure 12. The mean fraction of X–ray luminosity that arises from within the cooling radius is $\approx 25\%$, and there is no significant trend with velocity dispersion. There is clearly considerable scatter around this mean value, but this is comparable to the scatter in the calculated AGN heating rates shown in Figure 13, and so adoption of the mean value is reasonable. Combining this 25% fraction with the X–ray luminosity to velocity dispersion relation from Ortiz-Gil et al. (2004)[8] gives $L_{\rm X}(r < r_{\rm cool}) \approx 1.3 \times 10^{37} (\sigma_{\rm v}/1000{\rm km\,s^{-1}})^{4.1}{\rm W}$.

Figure 14 shows the fraction of the radiative cooling losses within the cooling radius that can be balanced by AGN heating from galaxies within that volume, assuming $f = 1$. Also shown are the location that the data points would occupy for alternative values of f. One conclusion is immediately apparent from these results: for a single value of f, radio-mode heating cannot balance radiative cooling losses for all systems from groups to clusters.

8 IMPLICATIONS FOR COOLING FLOWS

If radio–loud AGN heating is to exactly balance cooling in all systems, then the efficiency factor f must increase by a factor of 100–1000 between poor groups and rich clusters. As discussed in Section 7.2, the factor f includes any

[8] This is the middle-most of the four X–ray luminosity to velocity dispersion relations shown on Figure 13; these relations are fitted to a combination of (mostly) clusters and (a few) groups. There is no consensus in the literature as to how the slope of this relation changes for groups, and so here this mean relation is simply extrapolated down to the group regime; the conclusions of the paper would be unaffected even if the slope changed significantly below $300{\rm km\,s^{-1}}$ velocity dispersion.

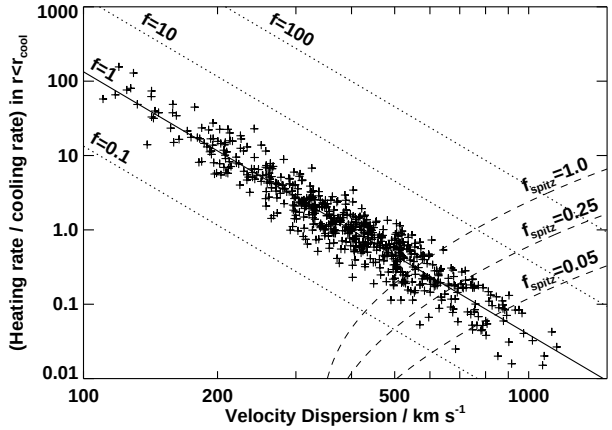

Figure 14. The data points show the ratio of the time–averaged heating rate associated with radio–loud AGN activity of all galaxies within the cooling radius, assuming $f = 1$ in Equations 3 and 4, to the radiative cooling losses within the cooling radius, as a function of cluster velocity dispersion. The solid line through these points, labelled '$f = 1$', represents the fit to these points. The dotted lines are scaled versions of this fit, showing where the data points would be located if $f = 0.1$, 10 and 100. Also shown (dashed lines) are estimates of the amount of heating that can be provided within the cooling radius by thermal conduction, assuming the radial temperature distribution of Allen et al. (2001), and different values of the suppression factor relative to the maximal Spitzer rate (see Section 8 for details).

uncertainty or variation in the conversion from radio luminosity to jet kinetic energy, and also in the efficiency with which the jet kinetic energy is used to heat the cluster within the cooling radius; either of these factors may be dependent upon environment. In the former case, any boosting of the radio luminosities of sources in richer environments due to confinement of the radio lobes would work in the opposite sense to that required to explain the trend in Figure 14. The efficiency of converting the radio source energy into heat, however, offers a more feasible environmental dependence of f. In the most massive clusters it seems quite reasonable that essentially all of the jet kinetic energy is used to heat the intracluster medium within the cooling radius of the cluster, since the cooling radius is large and observations indicate that shock/sound waves are efficiently produced. In smaller systems, however, the radio source heating may be more inefficient, either because of inefficient production of sound/shock waves or because the inflated bubbles rise beyond the cooling radius before much of their energy is transferred.

A lower efficiency of converting AGN energy into heat in smaller systems would help towards explaining the trend in Figure 14. However, given that radio–mode heating is dominated by low luminosity sources (Best et al. 2006), and such low luminosity sources tend to have small physical sizes, it seems unlikely that it can account for the required factor of 100–1000. If it does not, the conclusion has to be that it is the balance between AGN heating and radiative cooling which changes. In that case, either radio–loud AGN heating exceeds that required to balance cooling in groups (but matches in rich clusters; $f \sim 10$), or it falls short of that required in rich clusters (but matches that in groups; $f \sim 0.1$), or both ($f \sim 1$).

The possibility that the radio–mode heating in groups exceeds that required to balance cooling out to $r_{\rm cool}$ is interesting. The luminosity–temperature relation of groups is observed to have a steep slope ($L \propto T^5$; e.g. Helsdon & Ponman 2000), much steeper than the slope of 2 that would be expected from simple scaling laws for virialised gas, suggesting that the intra-group medium has also been heated by a non–gravitational energy source. The excess heating required corresponds to about 1keV per particle, and has been referred to as the 'entropy floor' (e.g. Ponman et al. 1999). One possibility is that the intra-group gas was pre–heated by supernovae from the early episodes of star formation in the group galaxies (e.g. Kaiser 1991; Balogh et al. 1999; Kay et al. 2003). However, to obtain sufficient energy from supernovae requires an extremely high efficiency of supernova feedback, and it is also difficult for such models to maintain consistency with the observed metallicity of that gas (e.g. Wu et al. 2000; Kravtsov & Yepes 2000). An alternative heating source, such as AGN, is therefore favoured (see the review by Mathews & Brighenti 2003, for a full discussion), and the overheating of the intragroup medium suggested here (for $f \gtrsim 0.1$) may provide this. Croston et al. (2005) found that the gas in galaxy groups containing radio–loud AGN is typically hotter than that in radio–quiet groups, providing a direct indication that radio–source heating can be very significant; more recently, however, Jetha et al. (2007) found no temperature difference in the very central regions of groups with and without radio sources, indicating that any radio source heating occurs preferentially at larger radii.

In order for radio–heating to balance cooling in the richest clusters, an efficiency factor $f \gtrsim 10$ is required. If all of the cavity enthalpy is used to heat the intracluster medium, and all of that heat is transferred within the cooling radius, then a value $f \approx 4$ is expected. If there is further heating from weak shocks, or errors in the mechanical luminosity determinations (e.g., significant heating from sources with extreme mechanical-to-radio luminosity ratios), then a still higher value could be obtained, and it may be possible to reach the efficiency required. Alternatively, an additional source of heating may be present in the most massive systems. The most likely process to provide this is thermal conduction, which will work to transport energy from the reservoir of hot gas outside the cooling radius down into the cooler cluster centre (e.g. Narayan & Medvedev 2001; Voigt et al. 2002; Zakamska & Narayan 2003; Voigt & Fabian 2004, and references therein). The heating rate due to thermal conduction was originally calculated for a pure hydrogen gas by Spitzer (1962), and on energy grounds alone thermal conduction at the maximal Spitzer rate can be sufficient to provide all of the heating necessary to balance cooling in some clusters (Voigt & Fabian 2004; Pope et al. 2006). However, in the presence of magnetic fields, thermal conduction will be suppressed; the amount of this suppression remains an open question, but Narayan & Medvedev (2001) argue that in the presence of turbulent magnetic fields it may be only a factor of a few. Fabian et al. (2006) support the argument that thermal conduction is relatively efficient in the inner regions of clusters, as this is necessary to explain why the shocks seen in the Perseus cluster are isothermal. Further, Reynolds et al. (2005) argue that viscosity at about

25% of the Spitzer value will make the radio bubbles in the intracluster medium stable against Rayleigh–Taylor and Kelvin–Helmholtz instabilities (although magnetic fields offer another possibility for providing this required stability; De Young 2003; Kaiser et al. 2005).

Thermal conduction can therefore play an important role in heating galaxy clusters. Voigt & Fabian (2004) and Pope et al. (2006) show, however, that thermal conduction cannot provide sufficient heating to balance cooling in all clusters, and nor does the radial distribution of the heating match that required. In particular, the temperature gradients in the inner regions of the clusters are too shallow to provide sufficient inward heat flux at the cluster centres (see also the discussion of Fabian et al. 2006, for the Perseus cluster). A combined model of AGN heating in the inner regions of the cluster, and heating by thermal conduction closer to the cooling radius, would solve this problem, however. Such a double–heating model was first developed by Ruszkowski & Begelman (2002), and has been shown to provide good agreement with observed cluster properties (see also Brüggen 2003; Hoeft & Brüggen 2004; Roychowdhury et al. 2005; Fujita & Suzuki 2005). The relative importance of thermal conduction should also increase in more massive clusters (Hoeft & Brüggen 2004), as would be required to account for the decreasing importance of AGN heating.

Allen et al. (2001) studied the temperature profiles of 6 relaxed clusters observed with Chandra, and found that all could be reasonable well–fitted using a universal temperature profile. Assuming that this profile is appropriate for all clusters[9] then the total flow of energy to within the cooling radius can be approximated, for different assumptions of the Spitzer suppression factor, $f_{\rm Spitz}$. These calculations are detailed in Appendix A, and the results are displayed on Figure 14: these confirm that for values of $f_{\rm Spitz} \approx 0.25$ thermal conduction could provide a large fraction of the necessary heating in the most massive clusters, but has little importance for clusters with velocity dispersions below 600–800 $\rm km\,s^{-1}$.

Finally, it is intriguing that for the expected values of $f \approx 1-4$, the combination of thermal conduction (with $f_{\rm Spitz} \approx 0.25$) plus AGN heating approximately balances cooling within the cooling radius for all systems larger than about 400 $\rm km\,s^{-1}$. In this scenario, at lower velocity dispersions the BCG radio–heating would exceed the radiative cooling losses within the cooling radius, and for systems with velocity dispersions below about 300 $\rm km\,s^{-1}$ it would exceed the radiative cooling losses of the entire intragroup or intracluster medium (not just that within the cooling radius). At this point, the radio source activity would lead to heating of the gas, possibly causing some of it to become unbound. This change in the gas properties may then account for the change in the luminosity–temperature relation between intragroup and intracluster gas that occurs at about 300–400 $\rm km\,s^{-1}$ velocity dispersion.

[9] The clusters studied by Allen et al. (2001) had velocity dispersions ranging from 800 to nearly 1500 $\rm km\,s^{-1}$, and so the validity of these calculations for systems with velocity dispersions much below 800 $\rm km\,s^{-1}$ is less certain.

9 CONCLUSIONS

The conclusions of this work can be summarised as follows:

- Brightest group or cluster galaxies of all stellar masses are more likely to host radio–loud AGN than other galaxies of the same mass. The probability of a BCG hosting a radio–loud AGN scales roughly linearly with stellar mass, which is shallower than the relation for all galaxies. BCGs are an order of magnitude more likely to host radio–loud AGN than other galaxies at stellar masses below $10^{11} M_{\odot}$, but less than a factor of two more likely at stellar masses above $5 \times 10^{11} M_{\odot}$.
- The distribution of radio luminosities of BCGs is independent of the mass of the BCG, and the same as that determined for other galaxies. Only the normalisation of the radio luminosity function changes, not its shape.
- The fraction of BCGs of a given stellar mass which host radio–loud AGN, and the distribution of their radio luminosities, do not depend strongly on the velocity dispersion of their surrounding group or cluster.
- Group and cluster galaxies other than the BCG show the same radio properties as those of field galaxies, except for those within $0.2 r_{200}$ of the centre of the system, which show a boosted likelihood of being radio–loud.
- The fraction of galaxies with emission–line AGN activity is smaller in all group and cluster galaxies within r_{200} than in field galaxies of the same mass. The suppression increases with decreasing cluster-centric radius, reaching a factor of 2–3 in the centre. With the exception of BCGs at the centre of strong cooling flow clusters, BCGs show the same emission–line AGN fractions as other galaxies of the same mass near the centre of the group / cluster.
- These results support the argument of (Best et al. 2005) that low–luminosity radio–loud AGN activity and emission–line AGN activity are independent physical phenomenon. It is argued that the radio–loud activity is associated with the cooling of gas from the hot envelopes of elliptical galaxies and, in the case of central cluster galaxies, also from the intracluster medium. Accretion of hot gas from a strong cooling flow is able to explain both the boosted likelihood of BCGs hosting radio–loud AGN, and the different slopes of the mass–dependencies of the radio–AGN fractions for BCGs and other galaxies.
- Within the cooling radius or a group / cluster, the mechanical heating output associated with BCG radio–AGN activity exceeds that of all other cluster galaxies combined.
- Either the mechanical–to–radio luminosity ratio or the efficiency of converting the mechanical energy of the radio source into heating the intracluster medium must be a factor 100–1000 higher in rich clusters than in poor groups in order that radio–AGN heating balances radiative cooling for systems of all masses. If not, then radio–loud AGN heating either overcompensates the radiative cooling losses in galaxy groups, providing an explanation for the entropy floor, and / or falls short of providing enough heat to counterbalance cooling in the richest clusters. Thermal conduction could provide the extra energy required in the richest clusters.

ACKNOWLEDGEMENTS

PNB would like to thank the Royal Society for generous financial support through its University Research Fellowship scheme. The authors thank the anonymous referee for numerous helpful comments. The research makes use of the SDSS Archive, funding for the creation and distribution of which was provided by the Alfred P. Sloan Foundation, the Participating Institutions, the National Aeronautics and Space Administration, the National Science Foundation, the U.S. Department of Energy, the Japanese Monbukagakusho, and the Max Planck Society. The research uses the NVSS and FIRST radio surveys, carried out using the National Radio Astronomy Observatory Very Large Array: NRAO is operated by Associated Universities Inc., under co-operative agreement with the National Science Foundation.

REFERENCES

Adelman-McCarthy J. K. et al. 2006, ApJ Supp., 162, 38
Allen S. W., Dunn R. J. H., Fabian A. C., Taylor G. B., Reynolds C. S., 2006, MNRAS, 372, 21
Allen S. W., Schmidt R. W., Fabian A. C., 2001, MNRAS, 328, L37
Bîrzan L., Rafferty D. A., McNamara B. R., Wise M. W., Nulsen P. E. J., 2004, ApJ, 607, 800
Baldwin J. A., Phillips M. M., Terlevich R., 1981, PASP, 93, 5
Balogh M. L., Babul A., Patton D. R., 1999, MNRAS, 307, 463
Barthel P. D., Arnaud K. A., 1996, MNRAS, 283, L45
Becker R. H., White R. L., Helfand D. J., 1995, ApJ, 450, 559
Benson A. J., Bower R. G., Frenk C. S., Lacey C. G., Baugh C. M., Cole S., 2003, ApJ, 599, 38
Bernardi M., Hyde J. B., Sheth R. K., Miller C. J., Nichol R. C., 2006, AJ submitted; astro-ph/0607117
Bernstein J. P., Bhavsar S. P., 2001, MNRAS, 322, 625
Best P. N., 2004, MNRAS, 351, 70
Best P. N., Kaiser C. R., Heckman T. M., Kauffmann G., 2006, MNRAS, 368, L67
Best P. N., Kauffmann G., Heckman T. M., Brinchmann J., Charlot S., Ž. Ivezić White S. D. M., 2005, MNRAS, 362, 25
Best P. N., Kauffmann G., Heckman T. M., Ž. Ivezić 2005, MNRAS, 362, 9
Blanton E. L., Sarazin C. L., McNamara B. R., Wise M. W., 2001, ApJ, 558, L15
Blanton M. R., Roweis S., 2007, AJ, 133, 734
Blanton M. R. et al. 2003, AJ, 125, 2348
Böhringer H., Voges W., Fabian A. C., Edge A. C., Neumann D. M., 1993, MNRAS, 264, L25
Bower R. G., Benson A. J., Malbon R., Helly J. C., Frenk C. S., Baugh C. M., Cole S., Lacey C. G., 2006, MNRAS, 370, 645
Brighenti F., Mathews W. G., 2006, ApJ, 643, 120
Brough S., Collins C. A., Burke D. J., Lynam P. D., Mann R. G., 2005, MNRAS, 364, 1354
Brüggen M., 2003, ApJ, 593, 700
Brüggen M., Kaiser C. R., 2002, Nat, 418, 301
Brüggen M., Ruszkowski M., Hallman E., 2005, ApJ, 630, 740
Burns J. O., 1990, AJ, 99, 14
Burns J. O., White R. A., Hough D. H., 1981, AJ, 86, 1
Carilli C. L., Perley R. A., Harris D. E., 1994, MNRAS, 270, 173
Cattaneo A., Dekel A., Devriendt J., Guiderdoni B., Blaizot J., 2006, MNRAS, 370, 1651
Churazov E., Brüggen M., Kaiser C. R., Böhringer H., Forman W., 2001, ApJ, 554, 261
Condon J. J., Cotton W. D., Greisen E. W., Yin Q. F., Perley R. A., Taylor G. B., Broderick J. J., 1998, AJ, 115, 1693
Croston J. H., Hardcastle M. J., Birkinshaw M., 2005, MNRAS, 357, 279
Croton D. et al. 2006, MNRAS, 365, 11
Dalla Vecchia C., Bower R. G., Theuns T., Balogh M. L., Mazzotta P., Frenk C. S., 2004, MNRAS, 355, 995
David L. P., Nulsen P. E. J., McNamara B. R., Forman W., Jones C., Ponman T., Robertson B., Wise M., 2001, ApJ, 557, 546
De Lucia G., Blaizot J., 2006, MNRAS, submitted; astro-ph/0606519
De Young D. S., 2003, MNRAS, 343, 719
Dunn R. J. H., Fabian A. C., Taylor G. B., 2005, MNRAS, 364, 1343
Edge A. C., 1991, MNRAS, 250, 103
Edwards L. O. V., Hudson M. J., Balogh M. L., Smith R. J., 2007, MNRAS, submitted
Fabian A. C., 1994, ARA&A, 32, 277
Fabian A. C., Sanders J. S., Allen S. W., Crawford C. S., Iwasawa K., Johnstone R. M., Schmidt R. W., Taylor G. B., 2003, MNRAS, 344, L43
Fabian A. C., Sanders J. S., Taylor G. B., Allen S. W., Crawford C. S., Johnstone R. M., Iwasawa K., 2006, MNRAS, 366, 417
Fabian A. C. et al. 2000, MNRAS, 318, L65
Fanaroff B. L., Riley J. M., 1974, MNRAS, 167, 31P
Finn R. A., Zaritsky D., McCarthy Jr. D. W., Poggianti B., Rudnick G., Halliday C., Milvang-Jensen B., Pelló R., Simard L., 2005, ApJ, 630, 206
Forman W. et al. 2005, ApJ, 635, 894
Forman W. et al. 2006, ApJ submitted; astro-ph/0604583
Fujita Y., Suzuki T. K., 2005, ApJ, 630, L1
Gómez et al. 2003, ApJ, 584, 210
Hatch N. A., Crawford C. S., Johnstone R. M., Fabian A. C., 2006, MNRAS, 367, 433
Heckman T. M., Baum S. A., van Breugel W. J. M., McCarthy P. J., 1989, ApJ, 338, 48
Heckman T. M., Kauffmann G., Brinchmann J., Charlot S., Tremonti C., White S. D., 2004, ApJ, 613, 109
Helsdon S. F., Ponman T. J., 2000, MNRAS, 315, 356
Hill G. J., Lilly S. J., 1991, ApJ, 367, 1
Hoeft M., Brüggen M., 2004, ApJ, 617, 896
Jetha N. N., Ponman T. J., Hardcastle M. J., Croston J. H., 2007, MNRAS, 376, 193
Kaastra J. S., Ferrigno C., Tamura T., Paerels F. B. S., Peterson J. R., Mittaz J. P. D., 2001, A&A, 365, L99
Kaiser C. R., Binney J., 2003, MNRAS, 338, 837
Kaiser C. R., Pavlovski G., Pope E. C. D., Fangohr H., 2005, MNRAS, 359, 493
Kaiser N., 1991, ApJ, 383, 104
Kauffmann G., White S. D. M., Heckman T. M., Ménard B., Brinchmann J., Charlot S., Tremonti C., Brinkmann

J., 2004, MNRAS, 353, 713
Kauffmann G. et al. 2003a, MNRAS, 341, 33
Kauffmann G. et al. 2003b, MNRAS, 341, 54
Kauffmann G. et al. 2003c, MNRAS, 346, 1055
Kay S. T., Thomas P. A., Theuns T., 2003, MNRAS, 343, 608
Khosroshahi H. G., Jones L. R., Ponman T. J., 2004, MNRAS, 349, 1240
Kravtsov A. V., Yepes G., 2000, MNRAS, 318, 227
Lauer T. R. et al. 2006, ApJ submitted; astro-ph/0606739
LaValley M., Isobe T., Feigelson E., 1992, BAAS, 24, 839
Ledlow M. J., Owen F. N., 1996, AJ, 112, 9
Lewis I. et al. 2002, MNRAS, 334, 673
Lin Y.-T., Mohr J. J., 2004, ApJ, 617, 879
Mahdavi A., Geller M. J., 2001, ApJ, 554, L129
Mateus A., Sodré L., 2004, MNRAS, 349, 1251
Mathews W. G., Brighenti F., 2003, ARA&A, 41, 191
Mathews W. G., Faltenbacher A., Brighenti F., 2006, ApJ, 638, 659
McNamara B. R., Nulsen P. E. J., Wise M. W., Rafferty D. A., Carilli C., Sarazin C. L., Blanton E. L., 2005, Nature, 433, 45
McNamara B. R. et al. 2000, ApJ, 534, L135
McNamara B. R. et al. 2006, ApJ, 648, 164
Miller C. J., Nichol R. C., Goméz P. L., Hopkins A. M., Bernardi M., 2003, ApJ, 597, 142
Miller N. A., Ledlow M. J., Owen F. N., Hill J. M., 2002, AJ, 123, 3018
Miller C. J. et al. 2005, AJ, 130, 968
Narayan R., Medvedev M. V., 2001, ApJ, 562, L129
Nipoti C., Binney J., 2005, MNRAS, 361, 428
Nusser A., Silk J., Babul A., 2006, astro-ph/0602566
Oemler A., 1976, ApJ, 209, 693
Omma H., Binney J., Bryan G., Slyz A., 2004, MNRAS, 348, 1105
Ortiz-Gil A., Guzzo L., Schuecker P., Böhringer H., Collins C. A., 2004, MNRAS, 348, 325
Peres C. B., Fabian A. C., Edge A. C., Allen S. W., Johnstone R. M., White D. A., 1998, MNRAS, 298, 416
Peterson J. R. et al. 2001, A&A, 365, L104
Ponman T. J., Cannon D. B., Navarro J. F., 1999, Nat, 397, 135
Pope E. C. D., Pavlovski G., Kaiser C. R., Fangohr H., 2006, MNRAS, 367, 1121
Popesso P., Biviano A., Böhringer H., Romaniello M., Voges W., 2005, A&A, 433, 431
Prestage R. M., Peacock J. A., 1988, MNRAS, 230, 131
Quilis V., Bower R. G., Balogh M. L., 2001, MNRAS, 328, 1091
Rafferty D. A., McNamara B. R., Wise M. W., Nulsen P. E. J., 2006, ApJ, submitted: astro-ph/0605323
Reynolds C. S., McKernan B., Fabian A. C., Stone J. M., Vernaleo J. C., 2005, MNRAS, 357, 242
Roychowdhury S., Ruszkowski M., Nath B. B., 2005, ApJ, 634, 90
Ruszkowski M., Begelman M. C., 2002, ApJ, 581, 223
Ruszkowski M., Brüggen M., Begelman M. C., 2004, ApJ, 611, 158
Scannapieco E., Silk J., Bouwens R., 2005, ApJ, 365, L13
Schombert J. M., 1986, ApJ Supp., 60, 603
Spitzer L., 1962, Physics of Fully Ionized Gases. Wiley, New York
Stoughton C. et al. 2002, AJ, 123, 485
Strauss M. A. et al. 2002, AJ, 124, 1810
Sun M., Forman W., Vikhlinin A., Hornstrup A., Jones C., Murray S. S., 2003, ApJ, 598, 250
Tamura T. et al. 2001, A&A, 365, L87
Tremaine S. et al. 2002, ApJ, 574, 740
Valentijn E. A., Bijleveld W., 1983, A&A, 125, 223
Voigt L. M., Fabian A. C., 2004, MNRAS, 347, 1130
Voigt L. M., Schmidt R. W., Fabian A. C., Allen S. W., Johnstone R. M., 2002, MNRAS, 335, L7
Voit G. M., Donahue M., 1997, ApJ, 486, 242
von der Linden A., Best P. N., Kauffmann G., White S. D. M., 2006, MNRAS, submitted; astro-ph/0611196
Wu K. K. S., Fabian A. C., Nulsen P. E. J., 2000, MNRAS, 318, 889
Xue Y.-J., Böhringer H., Matsushita K., 2004, A&A, 420, 833
Xue Y.-J., Wu X.-P., 2000, ApJ, 538, 65
York D. G. et al. 2000, AJ, 120, 1579
Zakamska N. L., Narayan R., 2003, ApJ, 582, 162

APPENDIX A: THE HEATING RATE DUE TO THERMAL CONDUCTIVITY

The volume heating rate due to thermal conductivity from an approximately infinite heat bath outside a radius r is given by

$$\epsilon = \frac{1}{r^2}\frac{\partial}{\partial r}\left(r^2\kappa\frac{\partial T}{\partial r}\right). \tag{A1}$$

where κ is the thermal conductivity of the gas and T is its temperature. Spitzer (1962) calculated the thermal conductivity for a pure hydrogen gas to be:

$$\kappa_{\rm S} = 1.84\times10^{-10}\frac{T^{5/2}}{\ln\Lambda}\,{\rm W\,m^{-1}\,K^{-1}} \tag{A2}$$

where $\ln\Lambda$ is the Coulomb logarithm. In the presence of magnetic fields, however, the thermal conductivity will be lower. This is usually accounted for by incorporating a factor $f_{\rm Spitz}$, such that

$$\kappa = \kappa_{\rm S} f_{\rm Spitz}. \tag{A3}$$

The Coulomb logarithm in Equation A2 depends weakly on the gas density and temperature, but to a good approximation can be treated as a constant with $\ln\Lambda \approx 37$ for typical conditions in clusters. Hence,

$$\kappa = \kappa_0 T^{5/2}, \tag{A4}$$

where $\kappa_0 \approx 5\times10^{-12} f_{\rm Spitz}$.

Allen et al. (2001) showed that the Chandra data of massive relaxed clusters could be fitted by a 'universal' temperature profile:

$$T = T_{2500}\left[T_0 + T_1\frac{(x/x_{\rm c})^\eta}{1+(x/x_{\rm c})^\eta}\right], \tag{A5}$$

where $T_0 = 0.40$, $T_1 = 0.61$, $x_{\rm c} = 0.087$ and $\eta = 1.9$ are dimensionless constants that they fitted to their data, T_{2500} is the temperature of the cluster gas at the radius r_{2500} (within which the mass density is 2500 times the critical density of the universe), and the dimensionless parameter x

is given by $x = r/r_{2500}$. Allen et al. (2001) assume $r_{2500} \approx 0.3 r_{200}$.

Substituting Equations A4 and A5 for κ and T into Equation A1 gives:

$$\begin{aligned}\epsilon \quad = \quad & \left\{ \eta T_1 T_{2500}^{7/2} \left(\frac{x}{x_\mathrm{c}}\right)^{\eta} \kappa_0 \left[T_0 + T_1 \left(1 - \frac{1}{1+(x/x_\mathrm{c}0)^{\eta}} \right) \right]^{0.5} \right. \\ & \left[T_0 + (T_0 + T_1) \left(\frac{x}{x_\mathrm{c}}\right)^{\eta} \right] \left[2\,(1-\eta)\,(T_0+T_1) \left(\frac{x}{x_\mathrm{c}}\right)^{2\eta} \right. \\ & \left. \left. + (4T_0 + (2+7\eta)\,T_1) \left(\frac{x}{x_\mathrm{c}}\right)^{\eta} + 2\,(1+\eta)\,T_0 \right] \right\} \Bigg/ \\ & \left\{ 2r^2 \left[1 + \left(\frac{x}{x_\mathrm{c}}\right)^{\eta} \right]^5 \right\}. \end{aligned} \tag{A6}$$

The total heating power due to thermal conduction inside a radius r is then roughly $4\pi r^3 \epsilon(r)/3$. Setting $r = r_\mathrm{cool}$, and using $r_\mathrm{cool} \approx 67(\sigma_\mathrm{v}/500\,\mathrm{km\,s^{-1}})\,\mathrm{kpc}$ from Section 7.3 then gives an approximation for the flow of heat to within the cooling radius.

In order to calculate this, r_{200} and T_{2500} are required. r_{200} can be estimated from the velocity dispersion as $r_{200} \approx 1230(\sigma_\mathrm{v}/500\,\mathrm{km\,s^{-1}})\,\mathrm{kpc}$ (from Finn et al. 2005, appropriate for redshift zero and the presently adopted cosmology). This then gives

$$x = 0.18 \left(\frac{\sigma_\mathrm{v}}{500\,\mathrm{km\,s^{-1}}} \right)^{-0.55}. \tag{A7}$$

Similarly, T_{2500} depends on the velocity dispersion, and can be estimated from the $T - \sigma_\mathrm{v}$ relation for clusters (Xue & Wu 2000):

$$T_{2500} \approx 2.4 \times 10^7 \left(\frac{\sigma_\mathrm{v}}{500\,\mathrm{km\,s^{-1}}} \right)^{1.56} K. \tag{A8}$$

Substituting for x and T_{2500} into Equation A6 allows the total heating rate within the cooling radius due to thermal conduction to be estimated, for different values of f_Spitz. Note that strictly these are only valid for systems with velocity dispersions $\sigma_\mathrm{v} \gtrsim 800\mathrm{km\,s^{-1}}$, since the 'universal' temperature profile of Allen et al. (2001) was only determined from massive clusters and may not fit lower mass systems. Nevertheless, it provides at least an indication of the likely importance of thermal conduction within systems of different masses, as shown on Figure 14.